Magnetic behavior of dense nanoparticle assemblies: Interplay of interparticle interactions and particle system morphology

G. Margaris,[1,2] K. N. Trohidou,[1] V. Iannotti,[3] G. Ausanio,[3] L. Lanotte,[3] and D. Fiorani[4]
[1]*IAMPPNM, Department of Materials Science, NCSR "Demokritos", Aghia Paraskevi, 15310 Athens, Greece*
[2]*Engineering Science Department, University of Patras, 26504, Greece*
[3]*CNR-SPIN and Department of Physical Sciences, University of Naples "Federico II", p.le V. Tecchio 80, I-80125 Napoli, Italy*
[4]*ISM–CNR, Area della Ricerca, Roma1, Via Salaria km 29.300, C.P. 10, 00016 Monterotondo Scalo (RM), Italy*
(Received 13 June 2012; revised manuscript received 11 December 2012; published 26 December 2012)

The role of interparticle interactions and the morphology in the magnetic behavior of dense assemblies of Fe nanoparticles with concentration well above the percolation threshold has been studied using the Monte Carlo simulations technique. The initial and temperature-dependent magnetization curves have been calculated for different conditions of the assembly morphology and the interparticle interaction strengths. Our simulations showed that the strong competition between the anisotropy and exchange energies in nonuniform dense assemblies results in a frustration of the nanoparticles moments coupling and creates plateaus and abrupt steps, which indicate a sudden, collective spin reversal, for low and intermediate dipolar strengths. In the case of strong dipolar interactions, the stepwise behavior becomes smoother and gradually disappears.

DOI: 10.1103/PhysRevB.86.214425 PACS number(s): 75.75.−c, 75.40.Mg, 75.30.Gw, 75.50.Tt

I. INTRODUCTION

In the continuous research effort for development of magnetic nanostructures with reduced size,[1] assemblies of interacting magnetic nanoparticles (NPs) have attracted a lot of interest because of the rapidly expanding areas of their applications, ranging from ultrahigh density recording media, quantum information devices to biomedicine.[2–5] Magnetic NPs are commonly formed in assemblies, with either random or ordered structure. Systems such as ferrofluids and granular solids belong to the first group, while patterned media (or magnetic dots) and self-assembled arrays of NPs belong to the second one. The macroscopic magnetic properties of these assemblies are very different from those of the bulk materials. The demand of the size minimization for technological applications requires dense assemblies and a small size of the NPs. Measurements in granular metals close to percolation have indicated the presence of intergranular exchange interactions with ferromagnetic character.[6]

In the assemblies of magnetic NPs, the crucial role of interparticle interactions in determining their response to an applied field and temperature has been recognized long ago.[7] When the interparticle interactions become significant, the system displays a rich variety of magnetic configurations, resulting from the competition between the different energy terms. In a disordered dense assembly of NPs, with randomly oriented magnetic moments, the dipolar interaction introduces frustration, as it is impossible to produce an optimal alignment for every particle. In addition, there is frustration resulting from the competition between the interparticle dipolar and exchange terms and the anisotropy energy that requires the magnetization vector to be aligned along specific axes in each particle.

A lot of effort has been concentrated on the understanding of the properties of uniform interacting assemblies with random anisotropy.[8,9] In these assemblies, when the particle density was above the percolation threshold, computer simulations including exchange coupling and dipolar interactions were performed,[10] showing that the coexistence of both types of interactions modifies the magnetic behavior of the assemblies as the density increases. The magnetic behavior of assemblies, with high single-particle anisotropy and weak interparticle exchange interactions[10–12] or low anisotropy energy in comparison with the exchange energy, has also been analyzed with mean field and analytical approaches,[11–14] using the random anisotropy model. These studies have demonstrated that different states of magnetic order arise, depending on the anisotropy-to-exchange ratio, which results in different magnetic properties. In the latter studies, dipolar interactions were not included.

Recently, there has been experimental activity on thin films, produced by femtosecond pulsed laser ablation[15] assisted by irradiation of the ablated NPs, in flight prior to deposition, with an appropriately delayed nanosecond ultraviolet (UV) laser beam.[16] The films consist of NPs with disklike shape. The very small particle size (smaller than 5 nm) and the high aspect ratio (most particles have a height of about 0.6 nm[17]) induce a high anisotropy, due to shape and surface contributions. Exchange interactions are reduced by the presence of voids between clusters of exchange-coupled particles.

The virgin curves (VCs)[17] and the temperature-dependent magnetization (Zero Field Cooling/Field Cooling[ZFC/FC]) curves (see Fig. S1 in the Supplemental Material[18]), exhibit a stepwise behavior, characterized by plateaus followed by rapid irreversible increments which are attributed to the existence of isolated particles and clusters. Stepwise behavior has been observed in other systems (phase-separated manganites,[19] intermetallic compounds,[20] metamagnets,[21] clean metals,[22] and molecular magnets[23]), but it is based on a different physical origin.

In this paper, we have developed a model of a nonuniform assembly of NPs with density well above the percolation threshold that includes explicitly the NPs' random anisotropies and the interparticle exchange and dipolar interactions considering the observed magnetic behavior in dense Fe thin films. We are using the Monte Carlo (MC) simulations technique

based on the Metropolis algorithm[24] to simulate a dense, random assembly in order to investigate the role of the morphology in the determination of the assembly's magnetic behavior. The various factors that influence the observed stepwise behavior are also being studied.

In Sec. II, we describe the structure of the model and the energy terms. In Sec. III, we discuss the results and identify the main factors that influence the magnetic behavior of the particle assembly. Our concluding remarks are presented in Sec. IV.

II. MODELS

We study the macroscopic behavior of an assembly of NPs, with randomly oriented magnetic moments.

To model the system, we consider N identical magnetic particles (grains) with spherical shape and diameter D. The magnetic particles are single-domain, and we represent them as three-dimensional classical unit spin vectors[25] with magnetic moment $\vec{m}_i = m_i\vec{s}_i,\ i = 1,\ldots,N$ of magnitude $m_i = M_s V_i$ and direction $\vec{s}_i$, with $|\vec{s}_i| = 1$, where M_s is the saturation magnetization and $V_i = \pi D^3/6$ is the particle volume. To each particle a uniaxial easy axis is assigned, randomly distributed.

In our calculations, we consider that the particles of the assembly are placed inside a box of edge lengths Lx, Ly, and Lz, on the nodes of a simple cubic lattice, with lattice constant a. In what follows, the box dimensions are $Lx = 12$, $Ly = 8$, and $Lz = 12$ measured in units of a. The total number of NPs is $N = p(LxLyLz)$, where p is the concentration of the particles in the system. The particles can touch each other, so there is direct exchange interaction between the neighboring particles. They also interact via long-range dipolar forces.

The total energy of the system is

$$E = \sum_i E_i, \tag{1}$$

where E_i is the energy per particle and is given by the sum of the Zeeman (due to interaction with an external field), the anisotropy, the exchange and the dipole-dipole interaction (DDI) energy terms, hence,

$$E_i = -\mu_0 m_i H(\vec{s}_i\hat{e}_h) - K_1 V_i(\vec{s}_i\hat{e}_i)^2 - \sum_{\langle i,j\rangle} J_{ij}\vec{s}_i\vec{s}_j - \frac{\mu_0 m_i}{4\pi a^3}\sum_{i>j} m_j\vec{s}_i D_{ij}\vec{s}_j, \tag{2}$$

where $\langle i,j\rangle$ denotes summation over nearest neighbors only, $\hat{e}_h$ and $\hat{e}_i$ are the directions of the magnetic field and the anisotropy axis of ith particle, respectively. The parameters entering Eq. (1) are the magnetic field H, the effective anisotropy constant K_1, and the effective exchange energy J_{ij}. The thermal energy is denoted by $E_T = k_B T$. Here, D_{ij} is the dipolar interaction tensor.

By rescaling all energy terms, we will use the anisotropy-reduced (dimensionless) parameters:

$$h = (\mu_0 M_s/K_1)H, \quad j_{ij} = J_{ij}/K_1 V, \quad g = \mu_0 M_s^2(D/\alpha)^3/24K_1, \quad t = (k_B/K_1 V)T, \tag{3}$$

for the magnetic field (h), the exchange interaction strength (j_{ij}), the DDI strength (g), and the temperature (t), respectively. In these reduced units, the anisotropy constant k is always 1.

For the single NP, the reduced energy is written as

$$\varepsilon_i = \frac{E_i}{K_1 V} = -h(\vec{s}_i\hat{e}_h) - k(\vec{s}_i\hat{e}_i)^2 - \sum_{\langle i,j\rangle} j_{ij}\vec{s}_i\vec{s}_j - g\sum_{i>j}\vec{s}_i D_{ij}\vec{s}_j. \tag{4}$$

We consider two types of morphologies, the one extracted from the experiments in Ref. 17 and the uniform assembly morphology.

In the first type of morphology, the input obtained from the experimental measurements is the following:

(a) the mean concentration of the particles is taken: $p = 0.5$;

(b) the NPs aggregate, forming clusters of few particles in contact (i.e. the interparticle distance is lower than the exchange correlation length) and big particles well separated from each other. In our model, for the simulation of the big particles, we consider small clusters very tightly exchange coupled. We call this model the nonuniform model of the assembly.

The Fe particles in the experimental samples are small oblate ellipsoids with an equivalent spherical median diameter $D = 2.6$ nm. The very small size and height (∼0.6 nm) and the peculiar particle morphology produced by fsPLD + UV, i.e. high aspect ratio (∼8) of disk-shaped NPs, indicates a considerable contribution of the surface and shape particle anisotropy energy to the total anisotropy energy.[17] The NP anisotropy constant has an effective value that includes surface, magnetocrystalline (bulk), and shape contributions. Typical values of the surface anisotropy are more than an order of magnitude greater than the bulk value,[26,27] so these contributions increase the effective particle anisotropy. For spherical Fe NPs with similar size, the anisotropy constant was found to be $K_{\mathrm{Fe}} = 2.4\times10^5$ J/m^3.[28] In our case, the particles produced by femtosecond pulsed laser deposition (fsPLD) + UV deposition systematically show a disklike shape, giving rise to a higher magnetic anisotropy, enhanced by shape and surface contributions.[17] Also, the average saturation magnetization M_s of the NP is expected to have a value smaller than the bulk iron value ($M_{s,\mathrm{Fe}} = 1.7\times10^6$ A/m), due to surface effects.[29]

Taking into account the above considerations, we expect that the dipolar interaction strength for the NPs is much smaller than the iron value for a spherical NP with $D = 2.6$ nm ($g_{\mathrm{Fe}} \sim 0.6$). So here, we consider $g = 0.1$.

Little information is available for the value of the effective exchange energy (j), and therefore, it is treated as a free parameter. The experimental VCs[17] and the ZFC/FC magnetization vs T curves (see Fig. S1 in the Supplemental Material[18]) show a collective reversal of the spins which produces a sudden change in the magnetization, indicating a strong competition between the anisotropy energy and the exchange energy, so the exchange coupling constant (j) must be comparable to the anisotropy constant (k). In addition, from the experiments, we know that the interparticle interaction between clusters of NPs is significantly reduced because of the presence of voids and some disordered oxide shell for particles lying on the film surface.[17]

In the real system, small variations of the interparticle distance (compared to the particle diameter D) result in a variation of the interparticle interaction strengths and especially of the short-range exchange interaction, which has strong dependence on the distance. So groups of particles form clusters of tightly connected particles. Particles that belong to different clusters interact with weaker exchange forces.

(c) In our model, for a dense assembly, the distance between two particles is at least one lattice spacing, which is equal to the particle diameter. In order to reproduce clusters of NPs and big isolated particles, we divide the lattice into eight areas with size $LxLyLz = 6 \times 4 \times 6$ each and a different particle concentration, but under the constraint that the total concentration will be $p = 0.5$. So the condition $p = (\sum_{i=1}^{n_a} p_i N_i)/N$ must be held, where $n_a = 8$ is the number of areas and N_i and p_i are the number of lattice sites and partial concentration in each area, respectively. As a result of the different concentrations in the areas, clusters of different sizes are formed in each of them. A schematic representation of our nonuniform model is given in Fig. 1. In Fig. 1(a), we give a 3D representation of the full model for $p = 0.5$, where the different colors of the NPs represent different areas. For a clearer picture, a 2D intersection at the $z = 3$ plane of our model is given Fig. 1(b).

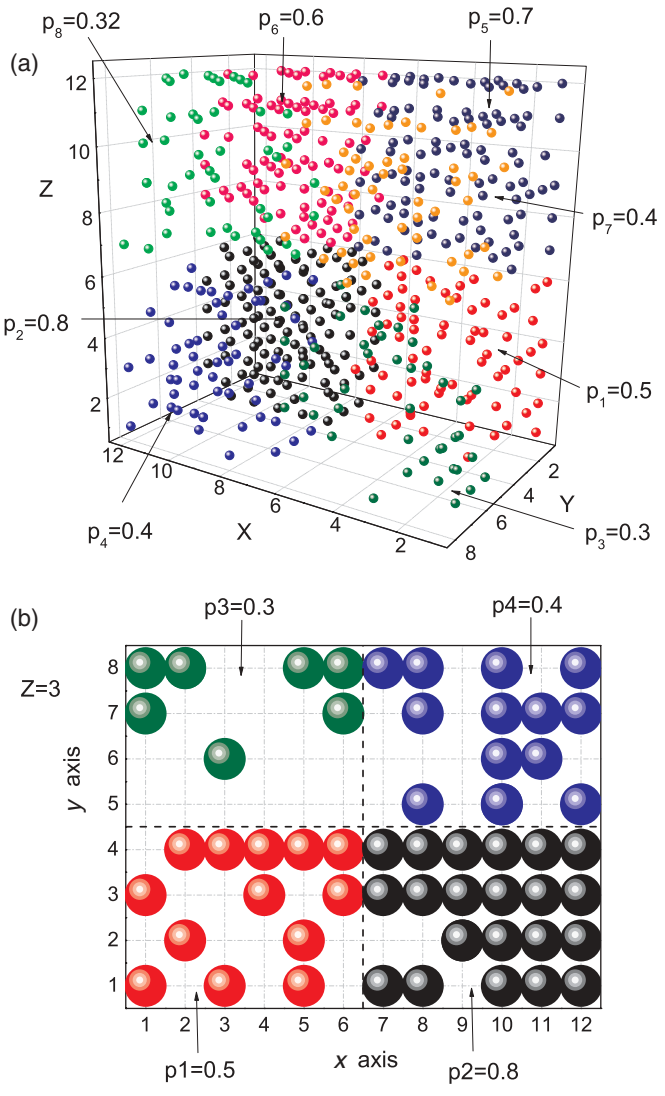

FIG. 1. (Color online) Schematic representation of the nonuniform assembly of NPs. (a) The three-dimensional sketch of the nonuniform assembly of NPs. (b) Two-dimensional vertical intersection of the nonuniform assembly at the $z = 3$ plane.

For the concentration $p = 0.5$, as in the experimental situation, we are well above the percolation threshold of the simple cubic lattice ($p_c = 0.3116$).[30] Some of these areas will be denser and some more diluted with partial concentrations smaller than the percolation threshold, so in some of them, more than one cluster will be formed. We consider that each particle interacts with exchange forces of the same strength with a nearest neighbor if they both belong in the same area. The number of the nearest neighbors of each particle (z_i) is a random variable, and the average value in each area is different and depends on its concentration ($z_{i,\mathrm{avg}} = 6p_i$). More specifically, p_i takes the values 0.50, 0.80, 0.30, 0.40, 0.70, 0.60, 0.40, and 0.32 in each of the eight areas, respectively. In the denser areas ($p_i \geqslant p$), the intracluster exchange interaction is $j = 1.0$ and in the more diluted ones ($p_i < p$) is $j = 8.0$ because, in this case, the whole cluster is considered to represent a bigger isolated particle. The exchange interaction strength between neighboring particles in different clusters is taken $j = 0.1$. In general, we assume a small intercluster exchange constant, which allows the cluster moments to be initially randomly oriented.

In order to investigate the effect of the morphology on the magnetic behavior of the assembly, we have considered a second model, consisting of a uniform assembly where the particles are placed randomly with an occupation probability $p = 0.5$ on the nodes of a simple cubic lattice with $Lx = 12$, $Ly = 8$, and $Lz = 12$. In this case, the exchange interaction strength j is constant, and the total number of particles is $N = p(Lx \times Ly \times Lz) = 576$.

The equilibrium spin configuration is obtained by the MC simulation technique, using the standard Metropolis algorithm.[24] For every field and temperature value, the first 500 steps per spin are used for equilibration, and the subsequent 5×10^3 are used to obtain thermal averages. The measurements are averaged over 10 different initial conditions (random configurations of the lattice occupied sites, anisotropy easy axis, and initial spin orientations). The error bars are very small, and they are not included in the figures.

Periodic boundary conditions are used, and the lattice is repeated periodically. We have implemented the Ewald summation technique for the calculation of the long-range dipolar interactions,[31,32] so the values of the dipolar interaction tensor (D_{ij}) are those of the Ewald matrix.

To study the magnetic behavior of the system, we calculate numerically the VC, where we plot the normalized magnetization as function of the field, and the ZFC/FC magnetization vs T curves, where the normalized magnetization is plotted as a function of the temperature. The calculated quantity is the normalized magnetization along the field direction, which is the z axis direction,

$$M_z/M_s = \frac{1}{NM_sV}\sum_{i=1}^{N} m_{iz} = \frac{1}{N}\sum_{i=1}^{N} s_{iz}. \qquad (5)$$

The simulation of the VC starts from the zero field at a given temperature. In the initial configuration, the spins are randomly oriented. The field is increased gradually until the assembly magnetization reaches saturation (M_z/spin ~ 1). The simulations are repeated at two different temperatures.

The simulations of the ZFC/FC magnetization vs T curves are performed in three steps. The first step is a simulated annealing process, starting from a temperature $T_{\max}$ much higher than the blocking temperature, so all the particles are in the superparamagnetic region. Then, the system is cooled down to a very low temperature ($t = 0.005$) at zero field ($h_{\text{cool}} = 0$). In the second step, a small cooling field is applied ($h_{\text{cool}} = 0.05$), the system is heated up slowly to the $T_{\max}$, and the ZFC/FC magnetization is recorded at several temperatures. In the third step, the temperature is gradually reduced down to the lowest value with the same cooling field, and the FC magnetization is recorded. All steps are performed at a constant temperature rate $\Delta T = 0.005$ every 5500 MC steps.

Before we present our simulation results, we have to note that the strong effective interparticle exchange coupling ($j \geqslant 1$) in an area and the uniaxial anisotropy result in a nonzero initial magnetization in each area, even in the absence of a field, after a few steps. This fact, and the small number of areas, may result in an initial average value of the magnetization different from zero. This deviation is of the order of $1/2\sqrt{n_a}$ (=0.176 for $n_a = 8$), under the condition that the interaction strength between the areas is weak. When the exchange interaction between particles in the different clusters is strong, the initial magnetization raises, and specific initial configurations have to be chosen to reduce the problem.[27]

III. RESULTS AND DISCUSSION

The behavior of the initial magnetization vs H curve and of the ZFC/FC magnetization vs T curve for the assembly with nonuniform morphology, as described in the previous section, has been experimentally demonstrated in Refs. 17 and 18, respectively. The experimental results showed a stepwise behavior in the VC and the ZFC/FC magnetization vs T curve. The stepwise behavior of the VC has also been confirmed by our MC simulations.[17]

Below we give a brief qualitative description of the mechanism that results in the experimentally observed VC,[17] in order to proceed with the physical description of the ZFC/FC curves' stepwise behavior.

In the calculation of the VC curves, initially the field just tilts the magnetic moments of some particles towards the field direction, overcoming their anisotropy energy. As the magnetization induced by the external field increases, an exchange field between the particles in a cluster is gradually built up which, at a certain value of the field, leads to a sudden reversal of the cluster moment. At higher fields, a higher order is established; there, clusters of strongly or even intermediate exchange coupled particles behave as big, single domain ferromagnetic particles with a small interparticle interaction. At very high fields, all the energy barriers have been overcome, leading to the full alignment of the clusters towards the field direction.[17]

In the ZFC/FC magnetization vs T curves, the mechanism of the initial plateau and the corresponding first step is similar to that of the VC. Initially, again, all particles remain in their blocked states almost randomly oriented, considering that the field is a small perturbation. At a certain temperature, the first energy barrier has been overcome. We must notice that, at the VC, this happens because, by increasing the field, we reduce the energy barriers; however, at the ZFC/FC magnetization vs T curve, the applied field is constant; therefore, the energy barrier does not change significantly (the temperature dependence of the anisotropy constant is not significant). By increasing the temperature, the stronger thermal fluctuations help the particle to overcome the energy barrier. As the temperature increases, the coupling between the most loosely coupled particles or clusters gradually becomes weaker, so some of them reverse without drifting their neighbors apart. In this way, we have a more gradual increase of the magnetization. At certain values of the temperature, as the ratios of the various energy constants with the temperature meet the proper conditions, we can have smaller jumps than those found at the second step of the VC.

In order to have a deeper insight into the magnetization behavior of our assembly, more specifically in the role of the morphology and the relative coupling strengths among the NPs, we examine the various factors that influence its behavior.

First, we study the concentration dependence of the nonuniform assembly. At lower concentrations, if the structure of the assembly is the same as in the dense nonuniform assembly case, we consider that a formation of clusters also occurs. We have performed simulations, keeping constant all the parameters of the dense assembly. By dividing the total and the partial concentrations with the same factor, we have

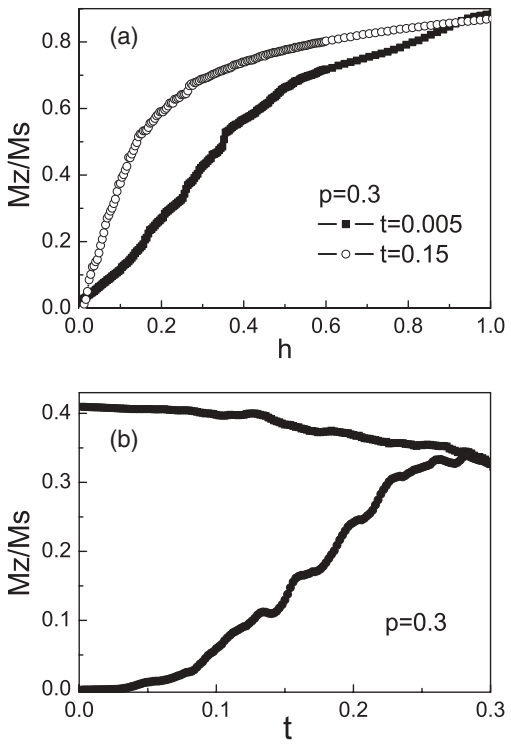

FIG. 2. (a) Initial magnetization vs H curves (VC) for two temperatures and (b) ZFC/FC magnetization vs T curves with $h_{\text{cool}} = 0.05$. The assembly concentration is taken $p = 0.3$.

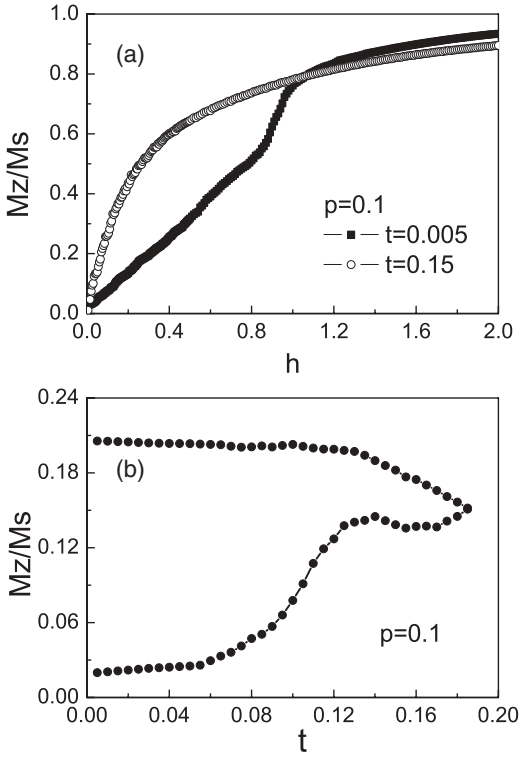

FIG. 3. (a) Initial magnetization vs H curves (VC) for two temperatures and (b) ZFC/FC magnetization vs T curves with $h_{\text{cool}} = 0.05$. The assembly concentration is taken $p = 0.1$.

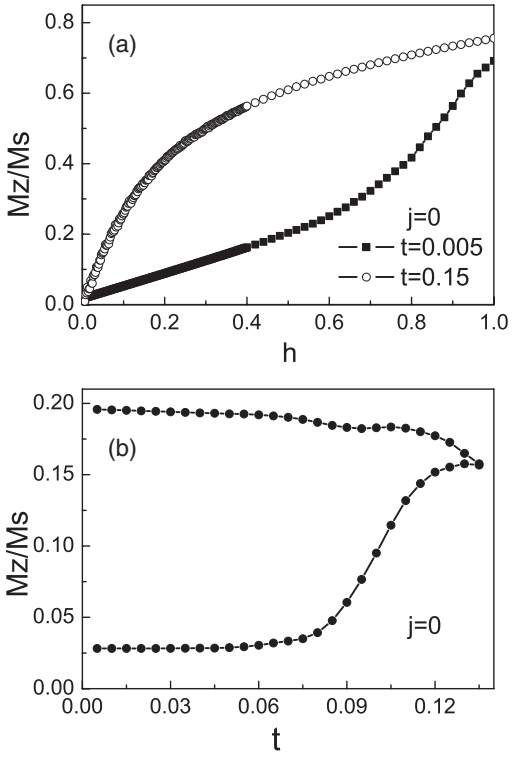

FIG. 4. Assembly of NPs interacting only via dipolar interactions with concentration $p = 0.5$. (a) Initial magnetization vs H curves (VC) for two temperatures and (b) ZFC/FC magnetization vs T curves with $h_{\text{cool}} = 0.05$.

calculated the VC and the ZFC/FC magnetization vs T curves for concentration $p = 0.3$ (Fig. 2) and $p = 0.1$ (Fig. 3).

For intermediate values of the total p ($p = 0.3 \sim p_c$), in most areas, the partial concentrations are still bigger than or close to the percolation threshold, so in such areas almost all particles form clusters, but now these clusters become smaller and more weakly coupled. In the remaining areas (the more diluted ones), either small clusters are formed, or we have isolated particles.

For dilute assemblies ($p = 0.1$) in all areas, p_i is much smaller than p_c, so only small clusters are formed. Most of the particles are isolated and interact only through dipolar interactions. In this case, we have a slower approach to saturation at the VC, and the average slope decreases [Figs. 2(a) and 3(a)]. Also, in the ZFC/FC magnetization vs T curves, the maximum occurs at lower temperatures [Figs. 2(b) and 3(b)]; consequently, the blocking temperature decreases in accordance with the findings of Ref. 10.

So, for small concentrations, the curves have similarities with those of noninteracting assemblies. However, some clusters are formed, so we see some small steps. At intermediate concentrations, more steps are present, but we have a gradual approach to saturation or maximum magnetization in the VC and ZFC/FC magnetization vs T curves, respectively (Fig. 3), so the abrupt steps of higher concentrations are not present. In particular, the VC has a larger slope at the initial plateau.

Next, we examine the role of the interparticle exchange interactions in the assembly. In our previous studies,[17] we have discussed the important role of the interparticle exchange interactions in the assembly on the observed step behavior. Here, we "switch off" the interparticle exchange interactions (i.e., $j = 0$), but we retain the dipolar interactions. As we can see in Fig. 4, the behavior of the assembly is completely different. Namely, in the pure dipolar case, steps do not exist, and the changes in the slope of the curves occur smoothly [Figs. 4(a) and 4(b)]. This behavior seen in Fig. 4 confirms the role of the interparticle exchange interaction in the stepwise behavior of the VC and the ZFC/FC magnetization vs T curves.

The role of the dipolar strength in the magnetization behavior of the assembly is examined next, in the case of a dense nonuniform assembly ($p = 0.5$). Dipolar interactions give rise to collective effects.[33,34] As the dipolar coupling increases, dipolar interactions start playing a more important role, start competing initially and gradually dominating over the exchange interactions and the anisotropy. In this case, we have a slower increase of the magnetization at low fields and a slower approach to saturation in the VC [Fig. 5(a)]. The local dipolar field is the sum of the fields of all the randomly oriented dipoles and oscillates randomly on every node. As a result, in some cases, reversals of clusters may create locally large dipolar fields, helping other spins or clusters to overcome their energy barrier and triggering their reversal more easily. These local fluctuations are larger as the dipolar strength increases. Consequently, smaller steps are present at different positions as the value of g increases [Figs. 5(a) and 5(b)]. We must notice here that, as it is expected, with the increase of the dipolar strength, we have an increase in the maximum of the ZFC/FC magnetization vs T curve. In Fig. 5(b), we see that, for $g = 0.8$, we do not observe the stepwise behavior. The

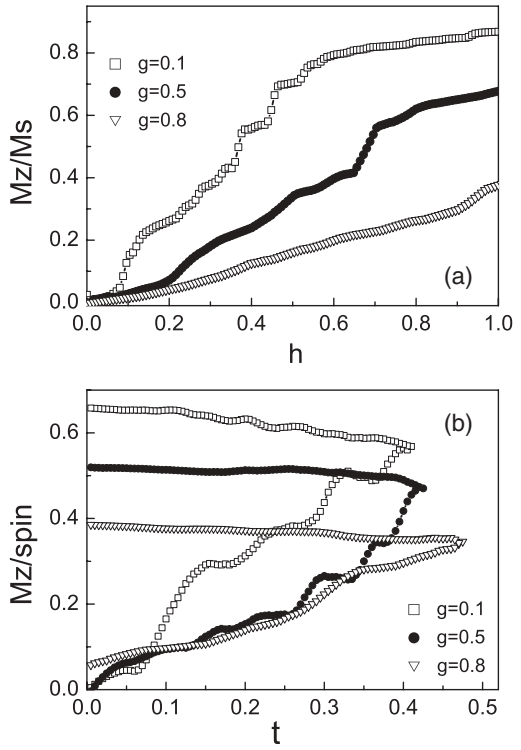

FIG. 5. Assembly of NPs interacting with three different dipolar interaction strengths (assembly concentration $p = 0.5$). (a) Initial magnetization vs H curves (VC) at temperature $t = 0.005$ and (b) ZFC/FC magnetization vs T curves with $h_{\text{cool}} = 0.05$.

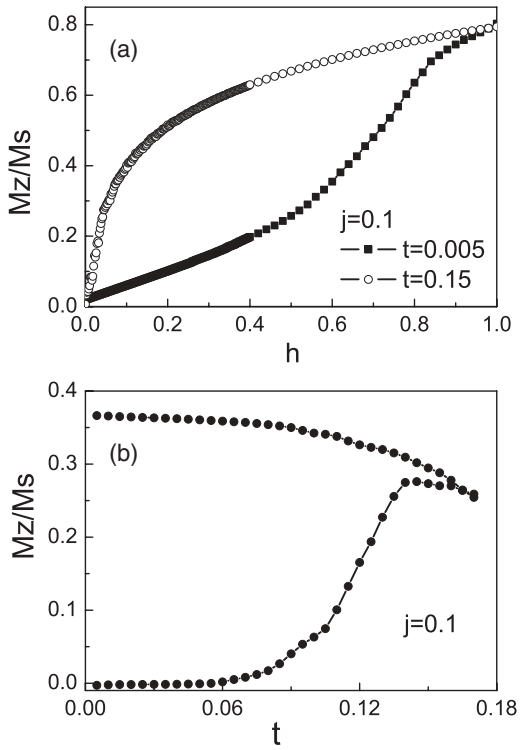

FIG. 6. Uniform assembly with $p = 0.5$ interacting with weak exchange forces ($j = 0.1$). (a) Initial magnetization vs H curves (VC) for two temperatures and (b) ZFC/FC magnetization vs T curves with $h_{\text{cool}} = 0.05$.

increase of g increases the dipolar field, and as a result, we need to apply a stronger cooling field.

We continue our study with the uniform morphology for the assembly of NPs. In this case, we distribute the particles at random on the nodes of the lattice with occupation probability $p = 0.5$. All particles interact via exchange interaction of the same strength and dipolar interactions.

We perform simulations for three different exchange interaction strengths, first with a weak exchange interaction strength ($j = 0.1 \ll k$), equal to the intercluster exchange interaction strength of the nonuniform assembly morphology. In this case, the curves are similar (in form and values) to those of nonuniform assemblies with a very low concentration, so no steps are present [Figs. 6(a) and 6(b)].

For a strong exchange interaction strength ($j = 8 \gg k$), all spins are tightly coupled. So the spins, coming from a random initial configuration, tend to align towards the same direction, along one of the effective, easy directions according to the random anisotropy model.[14] As the field or the temperature increases, we have a sudden reorientation of all the spins along the field, for the VC and ZFC/FC magnetization vs T curves, respectively. Consequently, in both cases, the transition from the initial to the final magnetization state occurs after a few values of the applied field or temperature, respectively [Figs. 7(a) and 7(b)].

Finally, when the exchange coupling constant is equal to the anisotropy constant ($j = k = 1$), there is a strong competition between the anisotropy energy and the exchange energy. The average assembly concentration is uniform, but density

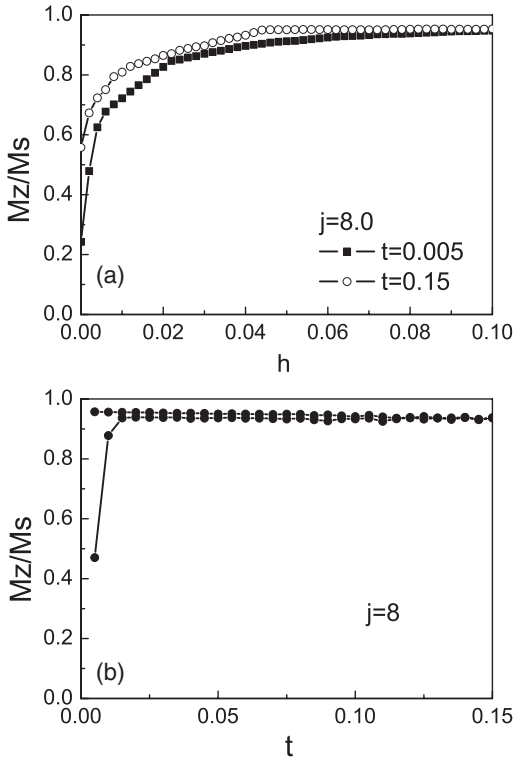

FIG. 7. Uniform assembly with $p = 0.5$ interacting with strong exchange forces ($j = 8$). (a) Initial magnetization vs H curves (VC) for two temperatures and (b) ZFC/FC magnetization vs T curves with $h_{\text{cool}} = 0.05$.

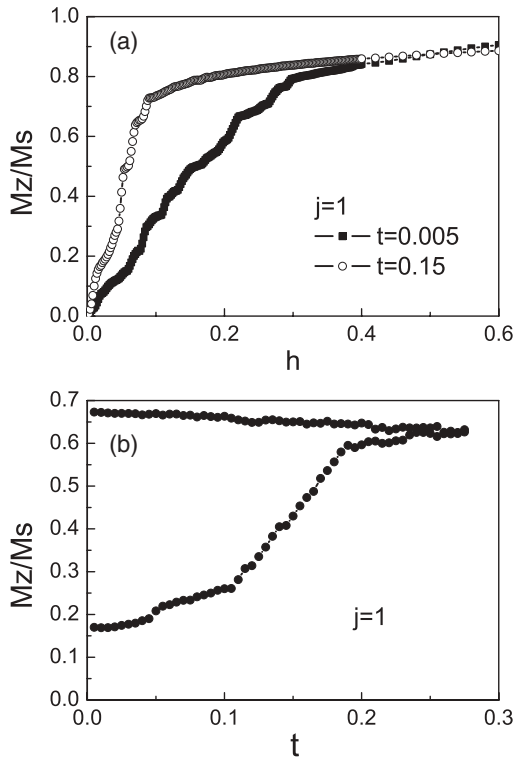

FIG. 8. Uniform assembly with $p = 0.5$ interacting with intermediate exchange forces ($j = 1$). (a) Initial magnetization vs H curves (VC) for two temperatures and (b) ZFC/FC magnetization vs T curves with $h_{\text{cool}} = 0.05$.

fluctuations may result in different local concentrations. As a result, we may have small agglomerates of particles more strongly connected in sites that have bigger numbers of neighbors and anisotropy axes towards the same direction. So smaller clusters, compared to the ones of the nonuniform morphology, are formed, but they are more strongly connected with other clusters or particles. We have to mention that, here, the definition of a cluster is different from that in the nonuniform model, as cluster in the nonuniform model is defined as a set of connected particles of the same area, each with coordination number $z_i \geqslant 1$, while here we require that $z_i \geqslant 3$. Steps in the curves may appear again [Figs. 8(a) and 8(b)], but smaller than those in the nonuniform assembly. Due to the simpler structure and to the stronger intercluster coupling, there are other differences, the larger initial magnetization in the ZFC/FC magnetization vs T curve, the larger initial slope, and stronger temperature dependence in the VC curves. This indicates again that the main source of the stepwise behavior, in random anisotropy models, is the competition between the exchange and anisotropy energy when they have comparable values, but the exact form of the initial plateau and steps is due to a more complicated structure where large clusters are formed.

IV. CONCLUSIONS

We have developed a model to study the magnetization behavior of a dense assembly of Fe NPs with nonuniform morphology as the one produced by fsPLD assisted by UV irradiation of the ablated NPs.[17] Using the MC simulations with the implementation of the Metropolis algorithm, we have investigated the various factors that influence the experimentally observed magnetic behavior of the assembly. Our simulations have shown that the creation of areas with different concentration results in the formation of clusters of different sizes and isolated particles and that magnetic behavior is determined by the system morphology. We found that the competition between the anisotropy energy and the exchange interaction with the voids at particle neighboring positions in the assembly results in a frustration of the NPs moments and produces a complicated energy landscape. Dipolar interparticle interactions play a minor role in the formation of a stepwise behavior for a wide range of dipolar strengths and affect only the collective behavior of the system. In the absence of interparticle exchange interaction, the steps disappear.

As the concentration decreases, the number and size of the clusters decrease, and smaller steps are present. As the system becomes more dilute, its behavior resembles that of noninteracting particles; however, steps do not disappear because, even at a small concentration, few clusters are formed.

The uniform assembly morphology results in a different magnetic behavior of the assembly. The steps disappear both at very strong and very weak exchange interaction strength, but for intermediate strength, some small steps exist, due to the random distribution of the NPs.

[1] V. Skumryev, S. Stoyanov, Y. Zhang, G. Hadjipanayis, D. Givord, and J. Nogues, Nature (London) **423**, 850 (2003).
[2] S. D. Bader, Rev. Mod. Phys. **78**, 1 (2006).
[3] Q. Pankhurst, J. Connolly, S. K. Jones, and J. Dobson, J. Phys. D **36**, 167 (2003).
[4] R. P. Cowburn and M. E. Welland, Science **287**, 1466 (2000).
[5] A. Imre, G. Csaba, L. Ji, A. Orlov, G. H. Bernstein, and W. Porod, Science **311**, 205 (2006).
[6] V. Franco, X. Batlle, A. Labarta, and K. O'Grady, J. Phys. D **33**, 609 (2000).
[7] J. L. Dormann, D. Fiorani, and E. Tronc, Adv. Chem. Phys. **98**, 283 (1997).
[8] D. Kechrakos and K. N. Trohidou, Appl. Phys. Lett. **81**, 4574 (2002).
[9] H. Kachkachi and M. Azeggagh, Eur. Phys. J. B **44**, 299 (2005).
[10] D. Kechrakos and K. N. Trohidou, J. Magn. Magn. Mater. **262**, 107 (2003).
[11] E. M. Chudnovsky, J. Appl. Phys. **64**, 5770 (1988).
[12] E. Callen, Y. J. Liu, and J. R. Cullen, Phys. Rev. B **16**, 263 (1977).
[13] R. Alben, J. J. Becker, and M. C. Chi, J. Appl. Phys. **49**, 1653 (1978).
[14] A. Hernando, P. Marın, M. Vazquez, J. M. Barandiaran, and G. Herzer, Phys. Rev. B **58**, 366 (1998).

[15]G. Ausanio, A. C. Barone, V. Iannotti, L. Lanotte, S. Amoruso, R. Bruzzese, and M. Vitiello, Appl. Phys. Lett. **85**, 4103 (2004); G. Ausanio, A. C. Barone, V. Iannotti, P. Scardi, M. D'Incau, S. Amoruso, M. Vitiello, and L. Lanotte, Nanotechnology **17**, 536 (2006).

[16]S. Amoruso, R. Bruzzese, X. Wang, G. Ausanio, and L. Lanotte, J. Phys. B: At. Mol. Phys. **40**, 1253 (2007).

[17]V. Iannotti, S. Amoruso, G. Ausanio, X. Wang, L. Lanotte, A. C. Barone, G. Margaris, K. N. Trohidou, and D. Fiorani, Phys. Rev. B **83**, 214422 (2011).

[18]See Supplemental Material at http://link.aps.org/supplemental/10.1103/PhysRevB.86.214425 for an experimental temperature-dependent magnetization (ZFC/FC) curve of a dense Fe thin film assembly.

[19]R. Mahendiran, A. Maignan, S. Hébert, C. Martin, M. Hervieu, B. Raveau, J. F. Mitchell, and P. Schiffer, Phys. Rev. Lett. **89**, 286602 (2002); G. Cao, J. Zhang, B. Kang, Y. Sha, S. Cao, and X. Shen, Europhys. Lett. **81**, 17003 (2008).

[20]V. Hardy, S. Majumdar, S. J. Crowe, M. R. Lees, D. McK. Paul, L. Herve, A. Maignan, S. Hebert, C. Martin, C. Yaicle, M. Hervieu, and B. Raveau, Phys. Rev. B **69**, 020407(R) (2004).

[21]H. Weitzel and J. Hirte, Phys. Rev. B **37**, 5414 (1988).

[22]G. Aeppli and Y. Soh, Science **294**, 315 (2001).

[23]L. Thomas, F. Lionti, R. Ballou, D. Gatteschi, R. Sessoli, and B. Barbara, Nature **383**, 145 (1996).

[24]K. Binder and D. W. Heermann, *Monte Carlo Simulation in Statistical Physics* (Springer-Verlag, Berlin, 1992).

[25]E. Stoner and E. Wohlfarth, Philos. Trans. R. Soc. London, Ser. A **240**, 599 (1948).

[26]F. Bødker, S. Mørup, and S. Linderoth, Phys. Rev. Lett. **72**, 282 (1994).

[27]D. A. Dimitrov and G. M. Wysin, Phys. Rev. B **54**, 9237 (1996).

[28]C. Binns, M. J. Maher, Q. A. Pankhurst, D. Kechrakos, and K. N. Trohidou, Phys. Rev. B **66**, 184413 (2002).

[29]B. D. Cullity and C. D. Graham, *Introduction to Magnetic Materials*, 2nd ed. (IEEE Press & Wiley, New Jersey, 2009).

[30]P. Grassberger, J. Phys. A **25**, 5867 (1992).

[31]R. Kretschmer and K. Binder, Z. fur Physik B **34**, 375 (1979).

[32]S. W. De Leeuw, J. W. Perram, and E. R. Smith, Proc. R. Soc. Lond. A **373**, 27 (1980).

[33]K. Nadeem, H. Krenn, T. Traussnig, R. Wuerschum, D. V. Szabo, and I. Letofsky-Papst, J. Magn. Magn. Mater. **323**, 1998 (2011).

[34]D. Parker, I. Lisiecki, C. Salzemann, and M. P. Pileni, J. Phys. Chem. C **111**, 12632 (2007).